JOURNAL OF THE PHYSICAL SOCIETY OF JAPAN, Vol. 41, No. 2, AUGUST, 1976

On the Exciton Luminescence at Low Temperatures: Importance of the Polariton Viewpoint

Hitoshi SUMI

Electrotechnical Laboratory, Tanashi, Tokyo 188

(Received December 15, 1975)

The intensity ratio of the LO-phonon sideband to the zero-phonon line and the width of the zero-phonon line in the free-exciton luminescence spectrum can never be understood, especially at low temperatures, by the usual theory with the assumption of the thermal equilibrium for excitons. The theory assuming exciton thermal-equilibrium gives too small values for these quantities compared with the observed ones. These large discrepancies are removed by considering the exciton luminescence from the polariton viewpoint. In this viewpoint, polaritons accumulate around the bottleneck in polariton decay lower a little than the lowest exciton energy E_0. Polaritons at the bottleneck determine the zero-phonon line, while polaritons maintaining approximately the thermal-equilibrium distribution in the energy region above E_0 determine the LO-phonon sideband. The temperature and crystal-thickness dependences of the luminescence spectrum and the quenching of the luminescence by impurities are also discussed in terms of the polariton bottleneck.

§1. Introduction

The free-exciton luminescence composed of the zero-phonon line and the LO-phonon sideband has been observed in many semiconductors and insulators.[1-3] It was pointed out by Gross *et al.* that the line shape of the LO-phonon sideband can well be fitted by the Boltzmann factor ($E^{3/2}\exp(-E/k_BT)$ for the one-LO-phonon sideband and $E^{1/2}\exp(-E/k_BT)$ for the two-LO-phonon sideband).[4] This seems to indicate that the thermal equilibrium of excitons is maintained during the luminescence process. In fact, Segall and Mahan could theoretically reproduce the intensity ratio between the one- and two-LO-phonon sidebands as well as their line shapes with the use of the assumption of the thermal equilibrium for excitons.[5]

However, it was pointed out by Segall and Mahan themselves that their exciton thermal-equilibrium theory could never explain the observed large width of the zero-phonon line.[5] Moreover, it was pointed out by the present author that the observed intensity ratio of the LO-phonon sideband to the zero-phonon line, which is usually of order unity, can never be explained by the assumption of the thermal equilibrium for excitons especially at low temperatures.[6] When the perturbation theory with respect to the exciton-photon interaction and the exciton-LO-phonon interaction is applied to excitons in thermal equilibrium, the intensity ratio mentioned above at temperature T much lower than the LO-phonon energy $\hbar\omega$ is given by

$$\sum_k \left|\frac{V_{op}(k)}{\hbar\omega}\right|^2 \exp\left[-(E_k-E_0)/k_BT\right], \quad (1.1)$$

where $V_{op}(k)$ is the matrix element of the exciton-LO-phonon scattering with momentum transfer k, and E_k and E_0 are respectively the exciton energies for momentum k and for zero momentum. With the use of the standard expression for $V_{op}(k)$,[7] it is easily shown that (1.1) is roughly estimated to be $(\Delta/\hbar\omega)(k_BT/\Delta)^{5/2}$ with the binding energy of exciton Δ. This theoretical value is very small compared with the observed one: For example, for the A exciton of CdS ($\hbar\omega\simeq 38$ meV and $\Delta\simeq 30$ meV), it is of order 10^{-5} at 4.2 K while the intensity ratio observed by Gross *et al.* is about two at 4.2 K.[4] The width of the zero-phonon line in the exciton thermal-equilibrium theory is determined by the exciton-acoustic-phonon interaction, and is about $10^{-2}\ k_BT$ for the A exciton of CdS.[5] This theoretical value is also very small compared with the observed half-width which is about 1 meV for $T\lesssim 10$ K.[4,8,9] The observed width can never be attributed to

the imhomogenious broadening by impurities since it is even larger than $k_B T$ for $T \lesssim 10$ K.

In a previous brief communication,[10] the present author pointed out that these large discrepancies mentioned above are removed in the polariton framework for the exciton luminescence. The polariton is the mixed mode of an exciton and a photon in a crystal.[11] High-energy polaritons excited initially fall down rapidly, interacting with phonons, almost along the exciton-like polariton branch with large density of states. This phonon-assisted decay, however, becomes less efficient towards the lowest exciton energy E_0 since the density of polariton states is very small below E_0. Instead, the radiative decay of polaritons in which polaritons escape the crystal through crystal boundaries as photons becomes efficient below E_0 with the use of the increasing photon component in the polariton state. Therefore, we see that the polariton decay has a bottleneck near E_0, as pointed out by Toyozawa.[12] In the polariton framework for the exciton luminescence, polaritons accumulating around the bottleneck determine the luminescence. The present polariton framework gives luminescence spectra different very much from those given by the previous exciton thermal-equilibrium theory especially at temperatures lower than the longitudinal-transverse splitting energy of exciton Δ_{LT}. The luminescence spectra depend on the crystal thickness in the polariton framework since the radiative decay of polaritons takes place only through crystal boundaries.

In the present work, the luminescence from the crystal excited steadily is calculated. The balance equation to determine the steady distribution of polaritons is derived in §2. Actual calculation is performed for the A exciton of CdS at temperatures lower than Δ_{LT}. The temperature dependence of the luminescence spectrum is shown in §3, and the crystal-thickness dependence in §4. Lattice defects such as impurities to trap excitons also deform the spectrum of the free-exciton luminescence as well as quench its intensity very much, at low temperatures, as shown in §5. Section 6 is devoted to discussions of further details.

§2. Balance Equation to Determine the Polariton Distribution

In this section, the phonon-assisted decay rate and the radiative decay rate of the lower-branch polariton are derived first, and then the balance equation to determine the steady distribution of polaritons in the lower polariton branch is constructed with them.

The polariton is the eigen mode of the Hamiltonian,

$$\sum_{k,\lambda}\left[\frac{\hbar c|k|}{\sqrt{\varepsilon}}a^{\dagger}_{k\lambda}a_{k\lambda}+E_k b^{\dagger}_{k\lambda}b_{k\lambda}+i\left(\frac{\pi\beta E_0^2 E_k}{\hbar c|k|\sqrt{\varepsilon}}\right)^{1/2}(b_{k\lambda}a^{\dagger}_{k\lambda}-b^{\dagger}_{k\lambda}a_{k\lambda}+b_{k\lambda}a_{-k\lambda}-b^{\dagger}_{k\lambda}a^{\dagger}_{-k\lambda})\right.$$
$$\left.+\frac{\pi\beta E_0^2}{\hbar c|k|\sqrt{\varepsilon}}(a_{k\lambda}a^{\dagger}_{k\lambda}+a^{\dagger}_{k\lambda}a_{k\lambda}+a_{k\lambda}a_{-k\lambda}+a^{\dagger}_{k\lambda}a^{\dagger}_{-k\lambda})\right],$$

which describes the interacting photon and transverse-exciton fields. Here, $a_{k\lambda}$ ($b_{k\lambda}$) is the annihilation operator of the photon (exciton) with momentum k, polarization λ and energy $\hbar c|k|/\sqrt{\varepsilon}$ (E_k). ε is the dielectric constant in the exciton-energy region and β is the polarizability of exciton. E_0 ($\equiv E_{k=0}$) is the lowest energy of the exciton band. The energy (E) and momentum (k) relation of the polariton which diagonalizes the Hamiltonian is determined by

$$\frac{\hbar^2 c^2 k^2}{E^2}=\varepsilon+\frac{4\pi\beta E_0^2}{E_k^2-E^2}\equiv n(E)^2, \qquad (2.1)$$

where $n(E)$ represents the refractive index of polariton. This equation gives two polariton energies E_1 and E_2 ($E_1<E_2$) for one momentum k; the lower and upper polariton branches. The annihilation operator of the polariton with momentum k, polarization λ and energy E_j ($j=1$ or 2) is written as

$$\alpha_{k\lambda j}=C_{j1}a_{k\lambda}+C_{j2}b_{k\lambda}+C_{j3}a^{\dagger}_{-k\lambda}+C_{j4}b^{\dagger}_{-k\lambda}. \qquad (2.2)$$

The coefficients $C_{j1}\sim C_{j4}$ are given in eq. (16) of ref. 11 in which $\hbar\omega_0$, $|k|$ and β should respectively be replaced by E_k, $|k|/\sqrt{\varepsilon}$ and $\beta E_0^2/\varepsilon E_k^2$. The polariton dispersion curve for the A exciton of CdS is shown in Fig. 1, where uses are made of the material constants (the isotropic effective mass for the exciton $=1.55\ m$, $\varepsilon=7$, $4\pi\beta=0.011$ and $E_0=2.55$ eV) which are

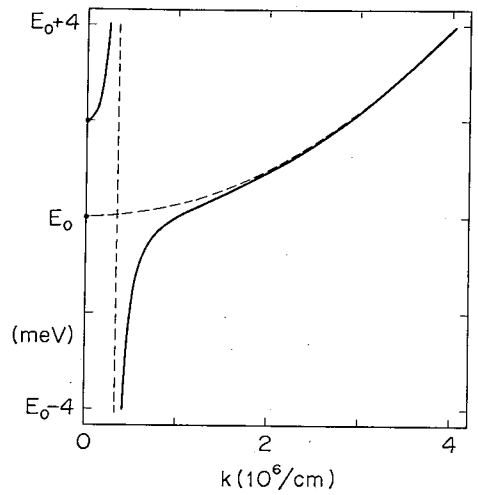

Fig. 1. Polariton dispersion relation appropriate for the A exciton of CdS. Dashed curves represent the unperturbed exciton and photon branches with the lowest exciton energy E_0. The solid curve starting from about E_0+2 meV represents the upper polariton branch and the other solid curve represents the lower polariton branch.

the same as adopted in ref. 13.

The polariton interacts with phonons through its exciton component and is scattered into other polaritons. The phonon-assisted decay of a lower-branch polariton takes place almost within the lower branch since the density of states is much larger in the lower branch than in the upper one. Now, we consider that the polariton with momentum k, polarization λ and energy E decays, when scattered by acoustic or optical phonons, into a polariton with momentum k', polarization λ' and energy E' within the lower polariton branch. In this case, the polarization λ' can be taken as being in the plane made by the momentum k' and the polarization λ. Therefore, the rate of the decay mentioned above at sufficiently low polariton densities is written as

$$W_\lambda(k, k')=\frac{2\pi}{\hbar}\sum_{i=\mathrm{ac,op}}|V_i(k-k')\Phi(k, k')\times\sin\theta(\lambda, k')|^2\{(n(\hbar\omega_{i,k-k'})+1)\times\delta(E-E'-\hbar\omega_{i,k-k'})+n(\hbar\omega_{i,k-k'})\times\delta(E-E'+\hbar\omega_{i,k-k'})\}, \quad (2.3)$$

with

$$\Phi(k, k')=\langle k'\lambda'|b^\dagger_{k'\lambda'}b_{k\lambda}+b^\dagger_{-k\lambda}b_{-k'\lambda'}|k\lambda\rangle. \quad (2.4)$$

Here, $V_{\mathrm{ac}}(q)$ ($V_{\mathrm{op}}(q)$) is the matrix element of the exciton scattering with the acoustic (optical) phonon with momentum q and energy $\hbar\omega_{\mathrm{ac},q}$ ($\hbar\omega_{\mathrm{op},q}$; $=\hbar\omega$). In the present case, we can confine ourselves to a small momentum transfer q such that $|q|$ is small compared with the inverse of the exciton Bohr radius since the polariton-phonon scattering in the energy region near the lowest exciton energy is important in the luminescence phenomena at low temperatures. Then, $V_{\mathrm{ac}}(q)$ and $V_{\mathrm{op}}(q)$ are written as[7]

$$\left.\begin{aligned}|V_{\mathrm{ac}}(q)|^2&=\frac{\hbar|q|D^2}{2V\rho u},\\ |V_{\mathrm{op}}(q)|^2&=\pi\left(\frac{\varepsilon_s}{\varepsilon_o}-1\right)\left(\frac{m_e-m_h}{m_e+m_h}\right)^2\frac{a_B^3}{V}\hbar\omega\frac{\hbar^2q^2}{2\mu},\end{aligned}\right\} \quad (2.5)$$

with the use of the crystal volume V, the density of the crystal ρ, the velocity of the LA phonon u, the deformation potential for the exciton D, the static (high-frequency) dielectric constant ε^s (ε_o), the effective mass of the electron (hole) m_λ (m_h), the exciton Bohr radius a_B, the LO-phonon energy $\hbar\omega$ and the reduced mass of the exciton μ. Here, a_B is defined by

$$\Delta=\frac{e^2}{2\varepsilon_s a_B}=\frac{\hbar^2}{2\mu a_B^2}, \quad (2.6)$$

with the use of the exciton binding energy Δ. In (2.3), $\theta(\lambda, k')$ represents the angle between the polarization λ and the momentum k', and $n(\hbar\omega)$ respresents the Bose-Einstein distribution function at temperature T. In (2.4), $|k\lambda\rangle$ represents the state in which the lower-branch polariton with momentum k and polarization λ is excited in the crystal. $\Phi(k, k')$ in (2.4) can be rewritten, with the use of the inverse transformation of (2.2)[11]

$$b_{k\lambda}=C^*_{12}\alpha_{k\lambda1}+C^*_{22}\alpha_{k\lambda2}-C_{14}\alpha^\dagger_{-k\lambda1}-C_{24}\alpha^\dagger_{-k\lambda2},$$

as

$$\Phi(k, k')=C_{12}(E)^*C_{12}(E')+C_{14}(E)^*C_{14}(E'), \quad (2.7)$$

where the energy dependence of the coefficients C_{ij} is explicitly shown. $\Phi(k, k')$ depends only on energies E and E'.

When the lower-branch polaritons are scattered by phonons into the energy region below or near the lowest exciton energy, the radiative decay of the polaritons takes place through their photon components. In the present work,

polaritons are assumed to be distributed uniformly in space and in momentum and polarization directions within the thin infinite slab with thickness L. Then, when a polariton with energy E is scattered by the crystal boundary with incident angle θ, the outgoing angle θ' of the photon emitted into the vacuum is determined by the classical electromagnetic theory as

$$\sin\theta' = n(E)\sin\theta, \tag{2.8}$$

with the use of the refractive index of polariton $n(E)$ in (2.1). In this case, the transmissivity of the incident polariton into the vacuum is given by

$$T(E,\theta) = 1 - \frac{1}{2}\left[\frac{\sin^2(\theta-\theta')}{\sin^2(\theta+\theta')} + \frac{\tan^2(\theta-\theta')}{\tan^2(\theta+\theta')}\right]. \tag{2.9}$$

Therefore, the radiative decay rate of a polariton with energy E is written as

$$P(E) = \frac{v(E)}{L}\int_0^{\theta_r} \sin\theta\cos\theta\, T(E,\theta)\,\mathrm{d}\theta, \tag{2.10}$$

where θ_r is the angle of total reflection determined by $n(E)\sin\theta_r = 1$ and $v(E)$ is the group velocity of the polariton. For the exciton-like polariton with energy above the lowest exciton energy, the refractive index $n(E)$ is much larger than unity and so the angle of total reflection is very small. Therefore, the exciton-like polariton can hardly escape the crystal.

Polaritons are trapped by lattice defects such as impurities and are changed into bound excitons, besides that they are scattered by phonons or escape the crystal as photons. Polaritons are trapped through their exciton components C_{j2} shown in (2.2), and the impurity-trapping rate of a lower-branch polariton with energy E can be written as

$$R(E) = R|C_{12}(E)|^2, \tag{2.11}$$

with R representing the impurity-trapping rate of an exciton.

With the use of (2.3), (2.10) and (2.11), the distribution function $\rho(E)$ for a polariton state with energy E in the lower polariton branch is determined by the balance equation as

$$\rho(E) = \frac{S(E) + \int_0^\infty W(E', E)g(E')\rho(E')\mathrm{d}E'}{P(E)+Q(E)+R(E)}, \tag{2.12}$$

where $S(E)$ represents the excitation rate and $Q(E)$ represents the phonon-assisted decay rate of a polariton with energy E defined by

$$Q(E) = \int_0^\infty W(E, E')g(E')\,\mathrm{d}E'. \tag{2.13}$$

Here, $g(E')$ is the density of polariton states per unit volume at energy E', and $W(E, E')$ is the phonon-assisted decay rate of a polariton with energy E into a polariton with energy E', given by

$$W(E, E')g(E')\mathrm{d}E' = \sum_{k'' \atop (E' < E'' < E' + \mathrm{d}E')} W_\lambda(k, k''), \tag{2.14}$$

with $W_\lambda(k, k'')$ in (2.3). Momenta k and k'' in (2.14) are respectively related with polariton energies E and E'' of the lower branch by (2.1). $g(E)$ is written as

$$g(E) = \frac{E^2}{2\pi^2\hbar^3c^2}\frac{n(E)^2}{v(E)}, \tag{2.15}$$

with the use of the polariton refractive index $n(E)$ in (2.1) and the polariton group velocity $v(E)$. The explicit form of $W(E, E')$ can easily be calculated with (2.14), but it is omitted here, except that we point out the relation

$$W(E, E')\exp(-E/k_BT) = W(E', E)\exp(-E'/k_BT), \tag{2.16}$$

which can also easily be proved.

The luminescence to be observed outside the crystal is determined by the polariton distribution function $\rho(E)$. The luminescence with energy E per unit time in a small solid angle $\mathrm{d}\Omega'$ around the outward normal of the crystal surface is given by

$$M(E)\mathrm{d}\Omega' = \left[1 - \left(\frac{n(E)-1}{n(E)+1}\right)^2\right]\rho(E)g(E)v(E)\frac{\mathrm{d}\Omega}{4\pi},$$

where $\mathrm{d}\Omega$ is the solid angle around the inward normal of the crystal surface determined by $\mathrm{d}\Omega'$ with (2.8). Therefore, with the use of (2.8) and (2.15), $M(E)$ is given by

$$M(E) = \frac{E^2}{8\pi^3\hbar^3c^2}\left[1 - \left(\frac{n(E)-1}{n(E)+1}\right)^2\right]\rho(E). \tag{2.17}$$

The excitation rate $S(E)$ in (2,12) is put as

$$S(E) \propto \delta(E - E_p), \tag{2.18}$$

where the excitation energy E_p is larger than the lowest exciton energy E_0.

Actual calculation is performed for the A exciton of CdS with the use of the electron effective mass $m_e=0.2\,m$, the density-of-states mass for the hole $m_h=1.35\,m$, the static dielectric constant $\varepsilon_s=8.87$, the high-frequency dielectric constant $\varepsilon_0=5.10$, the velocity of sound $u=4.4\times10^5$ cm/sec, the density of the crystal $\rho=4.82$ g/cm^3 and the LO-phonon energy $\hbar\omega=38$ meV which are the same as adopted in ref. 13. The deformation potential for the exciton is put at 2.5 eV, according to experiments.[5,14] In this case, it will be shown later that the polariton bottleneck is located at about $1\sim0.5$ meV below the lowest exciton energy E_0, with width about 1 meV, and that the polariton distribution with a peak at the bottleneck has a high-energy tail ranging up to about k_BT above E_0. Then, it can be shown that the polariton distribution near E_0 does not change with changing the excitation energy E_p of (2.18) if $|E_p-E_0-n\hbar\omega|$ is large enough compared with both of k_BT and 1 meV for any integer n. In this meaning, the luminescence spectrum dose not depend on the excitation energy.

§3. Temperature Dependence

The longitudinal-transverse splitting energy Δ_{LT} of the A exciton of CdS is about 2 meV as shown in Fig. 1. At low temperatures of $k_BT<\Delta_{LT}$, only the lower-branch polaritons contribute to the free-exciton luminescence. The present work is devoted to this low temperature case since discrepancies between the observed luminescence spectra and the usual exciton thermal-equilibrium theory are especially very large here. The crystal thickness L and the impurity-trapping rate R are fixed at $L=1$ μm and $R=0$ sec^{-1} in this section.

Figure 2(a) shows the polariton distribution function at energies around the lowest exciton energy E_0 for temperatures 0, 4 and 8 K, and Fig. 2(b) shows the zero-phonon line and the LO-phonon sideband in the luminescence spectrum which are calculated with the use of the distribution function. In Fig. 2(a), the thermal-equilibrium distribution function proportional to $\exp(-E/k_BT)$ is also shown for comparison. The polariton distribution functions shown in Fig. 2(a) have peaks at energies a little lower than E_0. This means that the polariton bottleneck is located a little lower than E_0. We note further in Fig. 2(a) that the distribution functions on the high-energy side of the distribution peaks are almost the same as the thermal-equilibrium distribution function at temperatures above about 4 K. The zero-phonon lines shown in Fig. 2(b) have widths about 1 meV and the intensity ratio between the zero-phonon line and the LO-phonon sideband is of order unity at the three temperatures. Therefore, the large discrepancies between the experiments and the usual exciton thermal-equilibrium theory mentioned in §1 are all

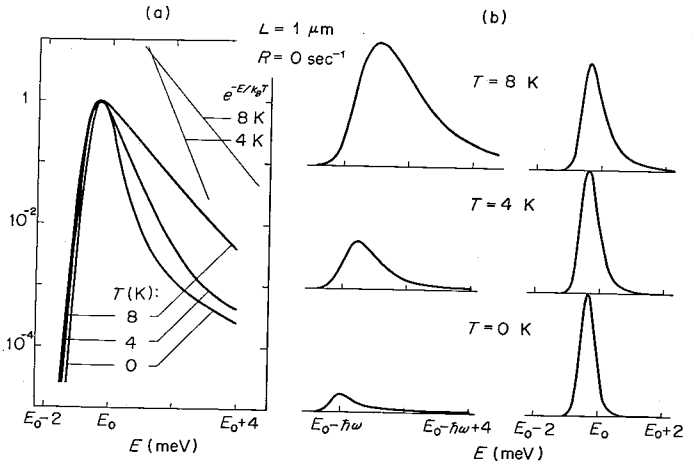

Fig. 2. (a) Distribution function for a lower-branch polariton state with energy around the lowest exciton energy E_0, and (b) The zero-phonon line (right) and the LO-phonon sideband (left) in the exciton luminescence spectrum. The crystal thickness and the impurity-trapping rate are respectively fixed at $L=1$ μm and $R=0$ sec^{-1} for the temperature $T=0$, 4 and 8 K. In (a), the thermal-equilibrium distribution function proportional to $\exp(-E/k_BT)$ is also shown.

removed in the present polariton framework.

The zero-phonon line shown in Fig. 2(b) is located at energies a little lower than E_0 and its width is almost determined by the width of the distribution peak at energies lower than E_0. The line shape of the LO-phonon sideband determined by (2.17) is almost determined by the energy dependence of the polariton distribution function $\rho(E)$ at energies around E_0-LO-phonon energy $\hbar\omega$ since the polariton refractive index $n(E)$ determined by (2.1) is almost equal to the energy-independent quantity $\sqrt{\varepsilon}$ in this energy region. Moreover, in this energy region, the radiative decay rate of polariton $P(E)$, which is much larger than the phonon-assisted decay rate $Q(E)$ here, is also almost energy independent because of the energy independence of the polariton refractive index. Therefore, the LO-phonon sideband spectrum is approximately proportional to

$$\int_0^\infty W(E', E)g(E')\rho(E')\mathrm{d}E',$$

for $E\simeq E_0-\hbar\omega$ with the use of (2.17) and (2.12). The integrand of this integral is large in the energy region of $E'>E_0$ where the polariton is almost exciton-like, since the polariton-phonon scattering rate $W(E', E)$ and the density of polariton states $g(E')$ are both much larger for $E'>E_0$ than for $E'<E_0$. The polariton distribution at energies larger than E_0 is almost the same as the thermal-equilibrium distribution at temperatures higher than about 4 K. Therefore, the line shape of the LO-phonon sideband in the present polariton framework is almost the same as that in the usual exciton thermal-equilibrium theory at temperatures higher than about 4 K, and is almost proportional to $(E-E_0+\hbar\omega)^{3/2}\times\exp[-(E-E_0+\hbar\omega)/k_BT]$.

§4. Crystal-Thickness Dependence

The radiative decay rate of polariton $P(E)$ in (2.10) is inversely proportional to the crystal thickness L, and so the luminescence spectrum depends on L. The polariton distribution functions and the luminescence spectra for $L=1$, 5 and 25 μm are shown in Fig. 3 where the temperature and the impurity-trapping rate are respectively fixed at $T=4$ K and $R=0$ sec^{-1}. With increasing L, the radiative decay rate decreases. Therefore, the polariton bottleneck becomes lower in energy with increasing L, and so do the peak of the polariton distribution function and the zero-phonon line as shown in Fig. 3. We note in Fig. 3(a) that the high-energy tail of the distribution function is almost the same as the thermal-equilibrium distribution function, independently on L. Therefore, the line shape of the LO-phonon sideband does not change with the change of L, as understood from the discussion in §3. The intensity ratio of the LO-phonon sideband to the zero-phonon line, however, increases with increasing L. This originates mainly from the increase of the

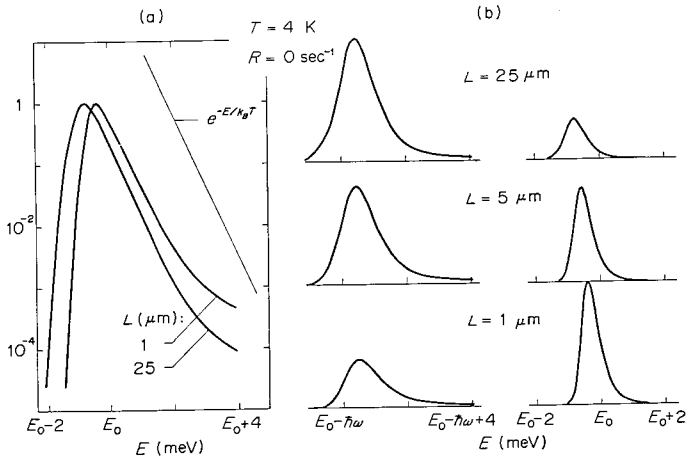

Fig. 3. (a) Distribution function for a lower-branch polariton state with energy around the lowest exciton energy E_0, and (b) The zero-phonon line (right) and the LO-phonon sideband (left) in the exciton luminescence spectrum. The temperature and the impurity-trapping rate are respectively fixed at $T=4$ K and $R=0$ sec^{-1} for the crystal thickness $L=1$, 5 and 25 μm. In (a), the thermal-equilibrium distribution function proportional to $\exp(-E/k_BT)$ is also shown.

distribution function $\rho(E)$ for $E \simeq E_0 - \hbar\omega$ due to the decrease of the radiative decay rate $P(E)$ with increasing L in the denominator of (2.12).

§5. Effect of Impurities

It has been known experimentalily that the free-exciton luminescence is quenched very much by the presence of lattice defects such as impurities especially at low temperatures. In the present polariton framework for the exciton luminescence, impurities play a role of trapping polaritons as bound excitons, as represented by (2.11). Figure 4 shows the effect of impurity trapping on the luminescence spectrum when the temperature T and the crystal thickness L are respectively fixed at 4 K and 1 μm. It should be noted that the excitation intensity of (2.18) is fixed in Fig. 4. Therefore, Fig. 4(a) shows that the polariton distribution peak near the lowest exciton energy E_0 is depressed with a small high-energy shift and the high-energy tail of this peak deviates from the thermal-equilibrium distribution, when the impurity-trapping rate R becomes larger than about 10^8 sec^{-1} at 4 K and $L=1$ μm. In parallel with these changes in the distribution function, the zero-phonon line and the LO-phonon sideband shift slightly to the high energy side as well as the intensity ratio of the latter to the former increases with increasing R. Moreover, it should be pointed out in Fig. 4(b) that intensities of these luminescence bands are depressed very much on the whole for $R \gtrsim 10^8$ sec^{-1} compared with those for $R=0$. This describes the quenching of the free-exciton luminescence by impurities.

§6. Discussion

First we discuss the polariton bottleneck. Energy dependence of the radiative decay rate of a polariton $P(E)$ and the phonon-assisted decay rate $Q(E)$ around the lowest exciton energy E_0 is shown in Fig. 5. The total decay rate of a polariton with energy E is $P(E)+Q(E)$ when the impurity-trapping rate vanishes. $P(E)+Q(E)$ makes a deep valley near $E=E_0$, as shown in Fig. 5, which is nothing but the polariton bottleneck. The total decay rate at the bottleneck is of order 10^8 sec^{-1} for $T \lesssim 8$ K and $L=1 \sim 25$ μm. Polaritons accumulating at the bottleneck gives rise to a peak of the polariton distribution near E_0 which is responsible for the zero-phonon line in the luminescence spectrum. This magnitude of the decay rate at the bottleneck agrees with the observed decay time[9] of the zero-phonon line which is several nano seconds at low temperatures.

For energies above the energy of the bottleneck, the phonon-assisted decay rate $Q(E)$ is large compared with the radiative decay rate $P(E)$ in (2.12). The Boltzmann factor of the polariton distribution function in this energy region mentioned before originates from the relation of the detailed balance (2.16) between polariton-phonon scattering rates.

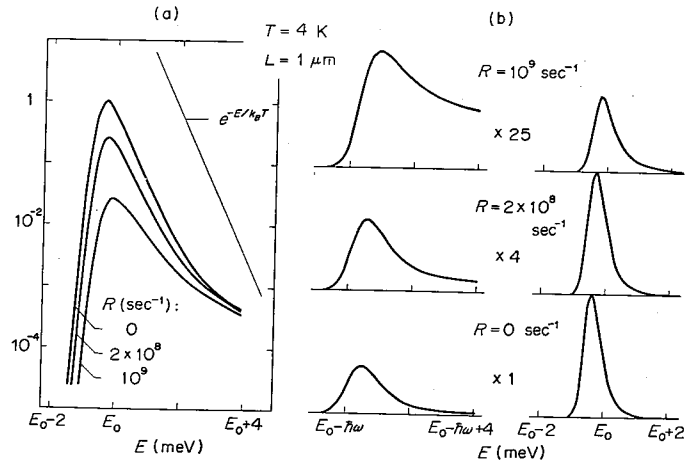

Fig. 4. (a) Distribution function for a lower-branch polariton state with energy around the lowest exciton energy E_0, and (b) The zero-phonon line (right) and the LO-phonon sideband (left) in the exciton luminescence spectrum. The temperature and the crystal thickness are respectively fixed at $T=4$ K and $L=1$ μm for the impurity-trapping rate $R=0$, 2×10^8 and 10^9 sec^{-1}. In (a), the thermal-equilibrium distribution function proportional to $\exp(-E/k_BT)$ is also shown.

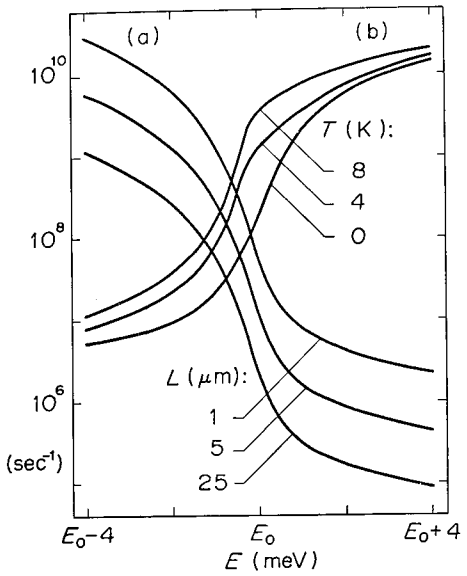

Fig. 5. (a) The radiative decay rate for the crystal thickness $L=1$, 5 and 25 μm and (b) the phonon-assisted decay rate for the temperature $T=0$, 4 and 8 K, of a lower-branch polariton with energy around the lowest exciton energy E_0.

When lattice defects such as impurities to trap polaritons are present, the total decay rate of a polariton is $P(E)+Q(E)+R(E)$ with the impurity-trapping rate $R(E)$ given by (2.11). $R(E)$ is proportional to $|C_{12}(E)|^2$, the square of the exciton amplitude in the polariton state, which is about

$$|C_{12}(E)|^2 \simeq \frac{\Delta_{LT}E_0/2}{(E-E_k)^2+\Delta_{LT}E_0/2}, \qquad (6.1)$$

for $|E-E_0| \ll E_0$, where Δ_{LT} is the longitudinal-transverse splitting energy of exciton and E_k is the exciton energy with mementum k which is determined by the polariton energy E with the dispersion relation (2.1). The quantity $\sqrt{\Delta_{LT}E_0/2}$ is about 50 meV for the A exciton of CdS. Therefore, $R(E)$ is almost equal to R, the impurity-trapping rate of an exciton, for E around the polariton bottleneck which is located at energies about $1 \sim 0.5$ meV lower than E_0 as shown in Fig. 5. When R is larger than the intrinsic decay rate $P(E)+Q(E)$ at the bottleneck which is about of order 10^8 sec^{-1} at low temperatures, impurities efficiently trap polaritons which gather to the bottleneck, and quench the free-exciton luminescence very much, as shown in §5. In this case, the impurity trapping takes place only in a narrow energy region around the bottleneck. This explains the experimental fact[15,16] that the excitation spectrum of the bound-exciton luminescence has a series of peaks at $E_0+n\hbar\omega$ for $n=0,1,2, \cdots$ with $\hbar\omega$ representing the LO-phonon energy. With increasing the crystal thickness L the intrinsic decay rate at the bottleneck decreases, as shown in Fig. 5, and the quenching of the free-exciton luminescence by impurities becomes more efficient. With increasing temperature, on the other hand, the intrinsic decay rate at the bottleneck increases, and the quenching becomes less efficient.

It was shown that the calculated intensity ratio of the LO-phonon sideband to the zero-phonon line is much larger in the present polariton framework than in the usual exciton thermal-equilibrium one. This cannot be interpreted as resulting from that the zero-phonon line is depressed very much because of the large refractive index of bottleneck polaritons with a strong exciton charactor at energies near E_0. The refractive index of polariton was given by (2.1) and can be rewritten as

$$n(E) \simeq \sqrt{\bar{\varepsilon}}\left(1+\frac{\Delta_{LT}}{E_k-E}\right)^{1/2}, \qquad (6.2)$$

for $|E-E_0| \ll E_0$ where Δ_{LT} and E_k represent the same as those in (6.1). For the A exciton of CdS, the zero-phonon line is about 0.5 meV lower than E_0 and Δ_{LT} is about 2 meV. Therefore, the enhancement of the refractive index at the zero-phonon line is not so large as to resolve the large discrepancies between the experiments and the usual exciton thermal-equilibrium theory. It should be noted here that polaritons responsible for the zero-phonon line are, in fact, almost exciton-like as understood from (6.1) but the enhancement of the refractive index is not very large at the zero-phonon line. In the present polariton framework for the exciton luminescence, the bottleneck polaritons responsible for the zero-phonon line come, by means of successive acoustic phonon scatterings, from the energy region of $E \gtrsim E_0$ with large density of states, while the polaritons with energies near $E_0-\hbar\omega$ responsible for the LO-phonon sideband come from the same energy region by means of the LO-phonon scattering. These acoustic phonon scatterings are very weak compared with the LO-phonon scattering, while the polariton lifetime is much longer at the

bottleneck than in the LO-phonon sideband region. Mutal compensation of these two effects results in that the intensity ratio of the zero-phonon line to the LO-phonon sideband is of order unity.

In the present work, the radiative decay rate $P(E)$ is calculated with the assumption that polaritons are distributed uniformly in the crystal with thickness L. Now, let E_m represent the energy below which $P(E)$ exceeds the phonon-assisted decay rate $Q(E)$ in Fig. 5, and let v_m and τ^{-1} represent respectively the polariton group velocity and the decay rate $P(E_m)+Q(E_m)$ $(=2P(E_m))$ at E_m. If $v_m\tau_m$ is larger than L, the assumption mentioned above is sufficiently justified. At 4 K, the value of $v_m\tau_m/L$ is about 64 for $L=1$ μm ($E_m\simeq E_0-0.5$ meV), about 42 for $L=5$ μm ($E_m\simeq E_0-0.7$ meV), and about 32 for $L=25$ μm ($E_m\simeq E_0-1.1$ meV). When impurities to scatter polaritons are present, the value mentioned above decreases more steaply with increasing L since the polariton bottleneck is more sensitive to impurities for larger L.

As shown in §5, the present work in the polariton framework can correctly explain that the free-exciton luminescence is quenched very much by impurities. If we assume the thermal equilibrium between the free excitons and the bound excitons, we could easily explain the quenching mentioned above without introducing the polariton bottleneck. However, we can show that the thermal equilibrium is not maintained between them at low temperatures: In order that the thermal equilibrium mentioned above is maintained, the condition that the current from free to bound excitons (or the reverse one) in the thermal equilibrium is much larger than decay currents of bound excitons into other modes than excitons must be satisfied, that is,

$$N'R'\exp\left(\frac{\Delta'}{k_BT}\right)\ll R\sum_k\exp\left(-\frac{\hbar^2k^2}{2m^*k_BT}\right),$$

where N', R' and Δ' are respectively the number of the impurities to trap excitons, the decay rate of the bound exciton mentioned above and the binding energy of the bound exciton. The effective mass of the free exciton is denoted by m^*. For CdS with a unit cell volume $\simeq 100$ (Å)^3 and $m^*\simeq 1.55\,m$, Δ' is estimated at the binding energy ($\simeq 7$ meV)[17] of the I_2 exciton bound by a neutral donnor with the decay rate R' of order 10^9 sec^{-1}.[9,18] Then, the condition at 4 K is written as

$$R\gg\frac{N'}{N}10^{23}\text{ sec}^{-1}, \tag{6.3}$$

with the number N of the unit cells in the crystal. Here, the impurity-trapping rate R should definitly be determined by the impurity concentration N'/N, and so we can examine in principle whether (6.3) is satisfied or not. In the real crystal, however, R is about the same in order as the decay rate of the free-exciton luminescence which is about $10^8\sim10^9$ sec^{-1},[9] and N'/N is much larger than 10^{-10}. Therefore, (6.3) is not satisfied. Then, we must consider such that the number of the bound excitons is much smaller than that determined by the thermal equilibrium between the free excitons and the bound excitons, and that the exciton (or polariton) current from the free excitons to the bound excitons is much larger than the reverse current, as assumed in §5.

Besides the polariton distribution peak at the bottleneck near the lowest exciton energy E_0, other distribution peaks in the lower-polariton branch exist at energies lower than the excitation energy E_p by any integral times the LO-phonon energy $\hbar\omega$, although they are not shown in Figs. 2$\sim$4 since their energies are much apart from E_0 except for the case $E_p-E_0\simeq n\hbar\omega$ for some integer n. These distribution peaks give rise to a series of luminescence peaks at $E_p-n\hbar\omega$ for any integer n, which correspond to the hot luminescence lines,[19,16] when polaritons in these distribution peaks (with energy E_n) escape the crystal as photons directly for $E_n<E_0$ or after scattered by phonons into the upper polariton branch for $E_n>E_0$. When $E_p-E_0\simeq n\hbar\omega$ for some integer n, one of the hot luminescence lines has an energy close to E_0, and the luminescence spectrum around E_0 and also those around $E_0-m\hbar\omega$ for any integer m are drastically changed. In fact, changes of the luminescence spectrum for $E_p-E_0\simeq n\hbar\omega$ have been observed by experiments.[20,9,16]

When k_BT is larger than the longitudinal-transverse splitting energy Δ_{LT}, scatterings of the lower-branch polaritons in thermal equilibrium above E_0 into the upper branch give rise to the polariton population in the upper branch, and this population contributes to the luminescence with energy larger than $E_0+\Delta_{LT}$. In fact,

the luminescence spectrum of CdS with $\Delta_{LT} \simeq$ 2 meV has two adjacent peaks around E_0 at about 20~30 K,[8,9] and the higher-energy peak seems to be attributed to the luminescence from the upper polariton branch.

Now, let us discuss previous works which treated the exciton luminescence in terms of polaritons. The theory by Tait and Weiher[13] is essentially almost the same as the theory with the assumption of the thermal equilibrium for excitons, although the reabsorption of the once emitted photon is taken into account. The point of their theory is essentially to consider that the photon with energy E emitted by excitons with a steady spacial distribution $D^{-1} \exp(-x/D)\,dx$ at $x \sim x+dx$ from the crystal surface reaches the crystal surface with probability $\exp[-\alpha(E)x]$, where D and $\alpha(E)$ represent respectively the effective diffusion length and the absorption coefficient of exciton. Then the luminescence spectrum $M(E)$ is given by

$$M(E) = \frac{K(E)}{D\alpha(E)+1}, \tag{6.4}$$

where $K(E)$ which is proportional to $\alpha(E) \times \exp(-E/k_B T)$ represents the luminescence spectrum without the reabsorption taken into account. Therefore, if $D\alpha(E)$ is much larger than unity in the zero-phonon-line region and is much smaller than unity in the LO-phonon-sideband region, the zero-phonon line is depressed strongly compared with that in $K(E)$. When the absorption spectrum around E_0 has a Lorentzian line shape, the intensity of the zero-phonon line in (6.4) is depressed by a factor $(D\alpha_m+1)^{-1/2}$ with α_m representing the maximum value of the absorption peak. For $D \simeq 10\,\mu$m and $\alpha_m \lesssim 10^6$ cm^{-1},[21] this factor can never compensate the large intensity ratio of the zero-phonon line to the LO-phonon sideband in $K(E)$ which is of order 10^5 at 4 K for CdS as pointed out in §1, and so this theory is inadequate at least at low temperatures. Bonnot and Benoit á la Guillaume[22] calculated the spacial distribution of polaritons as a function of the polariton energy E with the energy dependence of the polariton group velocity taken into account. In their theory, however, neither the radiative decay of polaritons through crystal boundaries nor the energy dependence of the phonon-assisted decay rate around E_0 is taken into account in determining the distribution function. Therefore, the polariton bottleneck as described in the present work is not taken into account there, and so their theory is inadequate to describe the polariton luminescence.

Acknowledgements

The author wishes to thank Professor Y. Toyozawa of the University of Tokyo for valuable discussions.

References

1) E. F. Gross, S. A. Permogorov and B. S. Razbirin: Soviet Physics-Uspekhi **14** (1971) 104.
2) T. Goto, T. Takahashi and M. Ueta: J. Phys. Soc. Japan **24** (1968) 314.
3) A. R. Lacey and L. E. Lyons: J. Chem. Soc. **1964**, 5393.
4) E. F. Gross, S. A. Permogorov and B. S. Razbirin: J. Phys. Chem. Solids **27** (1966) 1647.
5) B. Segall and G. D. Mahan: Phys. Rev. **171** (1968) 935.
6) H. Sumi: J. Phys. Soc. Japan **38** (1975) 825.
7) Y. Toyozawa: Progr. theor. Phys. **20** (1958) 53.
8) E. Gross, S. Permogorov, V. Travnikov and A. Selkin: Solid State Commun. **10** (1972) 1071.
9) U. Heim and P. Wiesner: Phys. Rev. Letters **24** (1973) 1205; P. Wiesner and U. Heim: Phys. Rev. **B11** (1975) 3071.
10) H. Sumi: Solid State Commun. **17** (1975) 701; J. Luminescence **12/13** (1976) 207 (Proc. 1975 Intern. Conf. Luminescence).
11) J. J. Hopfield: Phys. Rev. **112** (1958) 1555.
12) Y. Toyozawa: Progr. theor. Phys. Suppl. **12** (1959) 111.
13) W. C. Tait and R. L. Weiher: Phys. Rev. **178** (1969) 404..
14) J. E. Rowe, M. Cardona and F. H. Pollack: *II-VI Semiconducting Compounds*, ed. D. G. Thomas (Benjamin, New York, 1967) p. 112.
15) Y. S. Park and J. R. Schneider: Phys. Rev. Letters **21** (1968) 798; R. Planel, A. Bonnot and C. Benoit à la Guillaume: Phys. Status solidi **(b) 58** (1973) 251.
16) S. Permogorov: Phys. Status solidi **(b) 68** (1975) 9.
17) D. G. Thomas and J. J. Hopfield: Phys. Rev. **128** (1962) 2135.
18) J. J. Hopfield: *II-VI Semiconducting Compounds*, ed. D. G. Thomas (Benjamin, New York, 1967) p. 786.
19) R. C. C. Leite, J. F. Scott and T. C. Damen: Phys. Rev. Letters **22** (1969) 780.
20) E. F. Gross, S. A. Permogorov, V. V. Travnikov and A. V. Sel'kin: Soviet Physics-Solid State **13** (1971) 578.
21) M. S. Brodin and M. I. Strashnikova: Soviet Physics-Solid State **4** (1963) 1798.
22) A. Bonnot and C. Benoit à la Guillaume: *Polaritons*, ed. E. Burstein and F. De Martini (Proc. 1st Taormina Research Conf. on the Structure of Matter, 1972) (Pergamon, New York, 1975) p. 197.